THE JOURNAL OF BIOLOGICAL CHEMISTRY VOL. 282, NO. 5, pp. 2798–2807, February 2, 2007
© 2007 by The American Society for Biochemistry and Molecular Biology, Inc. Printed in the U.S.A.

A Novel Glycine Receptor β Subunit Splice Variant Predicts an Unorthodox Transmembrane Topology

*ASSEMBLY INTO HETEROMERIC RECEPTOR COMPLEXES**

Received for publication, September 19, 2006 Published, JBC Papers in Press, December 1, 2006, DOI 10.1074/jbc.M608941200

Jana Oertel[‡], Carmen Villmann[‡], Helmut Kettenmann[§], Frank Kirchhoff[¶], and Cord-Michael Becker[‡1]

From the [‡]Institut für Biochemie, Emil-Fischer-Zentrum, Universität Erlangen-Nürnberg, Fahrstrasse 17, 91054 Erlangen, Germany, the [§]Max-Delbrück-Centrum für Molekulare Medizin, Robert-Rössle-Strasse 10, 13092 Berlin, Germany, and the [¶]Max-Planck Institut für Experimentelle Medizin, Hermann-Rein-Strasse 3, 37075 Göttingen, Germany

The inhibitory glycine receptor is a ligand-gated ion channel with a pentameric assembly from ligand binding α and structural β subunits. In addition to α subunit gene variants (α1–α4) and developmental alterations in subunit composition of the receptor protein complex, alternative splicing of α subunits has been found to contribute to glycine receptor heterogeneity. Here, we describe a novel splice variant of the glycine receptor β subunit from mouse central nervous system, prevailing in macroglial cells, predominantly in astrocytes and extraneural tissues. As predicted by its cDNA sequence, the novel subunit βΔ7 lacks amino acid positions 251–302 encoded by exon 7 of the *Glrb* gene. Transcripts and antigen of βΔ7 were detected in cerebral cortex, liver, and heart. Lack of exon 7 results in a profoundly altered prediction of transmembrane topology as βΔ7 lacks TM1 and TM2 present in the full-length variant. Despite these topological alterations, *in vitro* studies showed that the βΔ7 polypeptide integrates into the plasma membrane, forming receptor complexes with the α1 subunit and gephyrin. Our data demonstrate that a topology deviating from the classical four transmembrane-fold is compatible with formation of glycine receptor protein complexes. However, co-expression of α1 with βΔ7 subunits did not change glycine receptor channel properties. Rather, the high level of expression in non-neuronal cells having intimate contact with synaptic regions may account for a yet unknown function of this splice variant βΔ7 in glycinergic neurotransmission.

Glycine receptors (GlyRs)[2] belong to the superfamily of Cys-loop receptors, which also include nicotinic acetylcholine receptors, ionotropic γ-aminobutyric acid receptors ($GABA_A$ and $GABA_C$), and the ionotropic serotonin receptor subtype $5HT_3$ (1). GlyRs are pentameric assemblies of five subunits surrounding a central ion-conducting pore that mediates rapid inhibitory neurotransmission in the spinal cord and brainstem (2, 3). Common features of all Cys-loop receptor subunits include four transmembrane regions (TM1–TM4), where TM2 forms the ion channel pore, and a large extracellular N-terminal ligand-binding domain. This domain shows significant structural homology to the acetylcholine-binding protein of *Lymnaea stagnalis* (4), a member of the immunoglobulin-like superfamily of proteins. By association of β subunits with the intracellular anchor protein gephyrin, GlyRs are clustered at the postsynaptic membrane. The gephyrin binding motif of the β subunit polypeptide has been mapped to the long intracellular TM3–4 loop (5–9).

The GlyR β subunit gene is widely transcribed throughout the central nervous system of neonatal and adult rodents. Starting at embryonic day 14, β transcripts are first detectable by *in situ* hybridization in rat spinal cord and telencephalon (10, 11). Expression of the ligand binding α subunit variants (α1–α4) is highly regulated during development (12, 13). Further GlyR subunit heterogeneity is generated by alternative splicing and RNA editing (α1 and α1ins; α2–3A and -3B; α3L and α3K) (11, 14, 15). Whereas, there are no reports about alternative splicing of the β subunit, aberrant splicing of GlyR β subunit transcripts underlies neurological disorders in a mouse mutant and human *hyperekplexia* (16). The pathological phenotype of the recessive mouse mutant *spastic*, where a LINE1 element is inserted into intron 5 of the *Glrb* gene results in exon skipping and a dramatic reduction in GlyR number (17, 18). Likewise, compound heterozygote mutations of the human β subunit gene *GLRB*, with one allele resulting in skipping of exon 5, cause the human neurological disorder *hyperekplexia* (16).

As evident from biochemical cross-linking experiments (3) and recombinant ion channel physiology (19) pentameric GlyRs display a subunit stoichiometry of $\alpha_2\beta_3$. Upon heterologous expression, however, GlyR α subunits are able to assemble into functional homopentameric channels in *Xenopus* oocytes or mammalian cells (10, 12, 20, 21). When co-expressed with α subunits, β subunits incorporate into heteromeric GlyRs and contribute to intracellular transport during protein biogenesis and receptor anchoring. Moreover, the β subunit modifies physiological and pharmacological properties of GlyR chloride channels as demonstrated by altered single channel conductance and induction of picrotoxin insensitivity of heteromeric α1/β as compared with homomeric α1 receptors (22–24). As a consequence of the interaction of the β subunit with gephyrin,

* This work was supported by Deutsche Forschungsgemeinschaft Graduiertenkolleg 805: Protein-Protein Interaktionen, SPP 1026 Molekulare Physiologie der synaptischen Interaktion, the Bundesministerium für Bildung und Forschung, and the Fonds der Chemischen Industrie. The costs of publication of this article were defrayed in part by the payment of page charges. This article must therefore be hereby marked "*advertisement*" in accordance with 18 U.S.C. Section 1734 solely to indicate this fact.

[1] To whom correspondence should be addressed. Tel.: 49-9131-852-4191; Fax: 49-9131-852-2485; E-mail: cmb@biochem.uni-erlangen.de.

[2] The abbreviations used are: GlyR, glycine receptor; Endo H, endoglycosidase H; RT, reverse transcription; NHS-S-S, sulfo-*N*-hydroxysulfosuccinimide; TM, transmembrane domain; GABA, γ-aminobutyric acid.

Downloaded from http://www.jbc.org/ by guest on September 27, 2016

GlyRs are clustered at the postsynaptic membrane. Gephyrin is highly enriched at the cytoplasmic face of the inhibitory postsynaptic membrane differentiations and colocalizes with both GlyRs and some $GABA_A$ receptor variants in spinal cord, retina, and other brain regions (25–29).

In this study, we identified by single cell RT-PCR a novel GlyR β subunit splice variant that lacks exon 7. This variant, termed βΔ7, is highly expressed in glial cells of rat spinal cord and in cultured astrocytes from mouse brain. The variant βΔ7 was also detectable in total RNA preparations from mouse spinal cord, cortex, liver, and heart. Exclusion of exon 7 predicts an altered transmembrane topology of the β polypeptide with TM1 and TM2 missing. Recombinant expression revealed that βΔ7 forms receptor complexes with the ligand binding α1 subunit as well as the anchor protein gephyrin.

EXPERIMENTAL PROCEDURES

Single Cell RT-PCR, Total RNA Extraction, and cDNA Synthesis and Amplification—Harvesting of cytoplasmic RNA, reverse transcription, and PCR were done as described (30, 31). In brief, patch clamp recordings were done and cellular RNA was harvested by applying negative pressure to the patch pipette filled with internal solution under visual control. Care was taken to avoid contaminations by material from adjacent cells. Immediately after retraction of the pipette, its content was expelled into a sterilized PCR tube containing 0.5 μl of 10 mM dNTPs (Roche), 1 μl of 50 μM random hexamer primers, 1 μl of 0.1 M dithiothreitol, and 0.5 μl of 30 units/ml RNasin (Promega). Reverse transcription was started by adding 0.5 μl of 200 units/μl of reverse transcriptase (Superscript II, Invitrogen) to a final volume of 10 μl. After incubation for 1 h at 37 °C, reaction was stopped by freezing at −20 °C.

The polymerase chain reaction was performed in a final volume of 50 μl containing 10 μl of reverse transcription reaction, 10 pmol, each, of sense and antisense primer, 5 μl of ×10 *Taq* polymerase buffer, and 2.5 units of *Taq* polymerase (Stratagene). A PerkinElmer Thermocycler 9600 was used set to 5 min at 94 °C for primary denaturation, 35–40 cycles for amplification (94 °C denaturation, 30 s; 45–51 °C annealing, 30 s; 72 °C elongation, 30 s (+1 s per cycle), and 10 min at 72 °C for elongation. After the final elongation step, PCR tubes were cooled to 4 °C and analyzed or frozen for later use. For detection of GlyRβ-specific cDNA sequences, two PCR were performed using different β specific primer pairs, bS1 and bAS1 in the first round, and "nested" primers (bS2/bAS2 generating DNA fragments of 509 bp length) in the second round. Primer sequences were bS1/bS2 (5′-GCTGCAGAGGACCTTGCCCGTGTGC-3′), bAS1 (5′-GCTCGAGCCACACATCCAGTGCCTT-3′), and bAS2 (5′-GTCGTCTTCGAACGTAGGACACTTTGGG-3′) (10). Due to interspersed intronic sequences, amplification of contaminating genomic DNA could be distinguished from amplified β cDNA fragments by the size differences of the respective amplimers. As a positive control, cDNA derived from spinal cord total RNA was used instead of cytoplasmic RNA from individual cells. For negative control, either buffer (internal pipette solution) was used instead of harvested RNA or cytoplasmic RNA obtained from glial cell displaying no glycine-evoked inward currents ($n = 3$). For sequencing, PCR amplification products were purified and cloned into pBluescript (Stratagene).

Total RNA extractions were performed from astrocytes, spinal cord neurons, and different tissues (cortex, spinal cord, heart, and liver) from C57BL/6J mice (Jackson Laboratories). Following lysis using *PeqLab Gold* solution (PeqLab, Erlangen), the RNA was precipitated with chloroform and isoamyl alcohol. Finally, the RNA was washed twice with ethanol (75%) and dried on ice. cDNA synthesis was done as described above. PCR conditions differed only in the annealing temperature (60 °C). The expected amplimer sizes were 606 bp for the β subunit and 453 bp for βΔ7. Primer sequences used for amplification of β or βΔ7 are: bD7S (5′-TTGGATATACAACCGATGATTT-3′), bD7AS (5′-TTGCATCTGGTCTCACCAAC-3′); for β-actin amplification sense (5′-TGAGACCTTCAACACCCCAG-3′), antisense (5′-CATCTGCTGGAAGGTGGACA-3′). PCR amplimers were verified by restriction digests and sequencing (ABI sequencer).

Transfection of HEK293 and COS7 Cells—COS7 cells were transfected (10 μg of plasmid/10-cm dish) using DEAE-dextran (10 mg/ml). HEK293 cells were transiently transfected (10 μg of plasmid/10-cm dish) using a modified calcium-phosphate precipitation method (32). Green fluorescent protein was cotransfected as a control for transfection efficiency. All experiments for immunocytochemistry, protein biochemistry, and electrophysiological recordings were performed 48 h following transfection. For glycosylation analysis, tunicamycin (5 μg/ml) was added 5 h after transfection, and the cells were incubated in the presence of tunicamycin for an additional 24 h prior cell lysis.

Electrophysiological Analysis of Spinal Cord Glia and Transfected HEK293 Cells—Preparation of spinal cord slices and electrophysiological setup were done as described previously (30). For recordings, cells were selected that were located 10–30 μm below the surface of the slice and displayed a clear, dark membrane surface. Membrane currents were measured applying the patch clamp technique in a whole cell recording configuration (33). During application of a series of de- and hyperpolarizing voltage steps (50 ms, ranging from −160 to +20 mV in 10-mV increments), whole cell membrane currents were recorded and cells were classified as astrocytes, oligodendrocytes, or glial progenitor cells/NG2 glia (30, 34). Current signals were amplified with conventional electronics (EPC-7 or EPC-9 amplifier, HEKA), filtered at 3 kHz, and sampled at 5 kHz. A standard bathing solution was used in the experiments with the following composition: 134.0 mM NaCl, 2.5 mM KCl, 2.0 mM $CaCl_2$, 1.3 mM $MgCl_2$, 1.25 mM K_2HPO_4, 26.0 mM $NaHCO_3$, 10.0 mM D-glucose, pH 7.4 (a total K^+ concentration of 5 mM). The solution was gassed with a mixture of 95% O_2 and 5% CO_2. The internal pipette solution was composed of: 130.0 mM KCl, 0.5 mM $CaCl_2$, 3.0 mM $MgCl_2$, 5.0 mM EGTA, 10.0 mM HEPES, pH 7.2.

Whole cell recordings from transfected HEK293 cells were performed by application of ligand (100 μM glycine) or coapplication of ligand together with picrotoxin (100 μM) using a U-tube that bathed the suspended cell in a laminar flow of solution, giving a time resolution for equilibration of 10–30 ms. The external buffer consisted of 137 mM NaCl, 5.4 mM KCl, 1.8 mM $CaCl_2$, 1.0 mM $MgCl_2$, 5.0 mM HEPES, pH adjusted to 7.2 with

Downloaded from http://www.jbc.org/ by guest on September 27, 2016

NaOH; the internal buffer was 120 mM CsCl, 20 mM $N(Et)_4Cl$, 1.0 mM $CaCl_2$, 2.0 mM $MgCl_2$, 11 mM EGTA, 10 mM HEPES, pH adjusted to 7.2 with CsOH. Current responses were measured at a holding potential of −60 mV. All experiments were carried out at room temperature. Recording pipettes were fabricated from borosilicate capillaries. The open resistance of these patch pipettes was 5–6 megohms.

Biotinylation of Cell Surface Protein and in Vitro Deglycosylation—The biotinylation assay was performed 48 h post-transfection of COS7 cells grown in 6-cm dishes as described previously with little variations (35). In brief, after labeling of surface protein with EZ-link™ sulfo-(NHS)-S-S biotin (Pierce) and cell lysis, supernatants were incubated with 50 μl of streptavidin-Sepharose beads (Sigma) for 4 h at 4 °C while rotating. Biotinylated proteins were eluted by boiling the probes in 1× sample buffer for 5 min. For Endo H digest, biotinylated surface proteins were denatured in 1× denaturing buffer at 100 °C for 10 min, Endo H (New England Biolabs) digest was done following the manufacturer's protocol.

Antibody Generation—A peptide epitope bridging the border of exons 6 and 8 within the βΔ7 sequence (TKYYK-GTGIFSVLSLASECEC) was chosen based on antigenicity prediction. The peptide was synthesized using Fmoc (*N*-(9-fluorenyl)methoxycarbonyl)-PAL-PEG-PS-resin to construct a peptide-amide (9050 PlusPep Synthesizer, Millipore). The integrity and purity of the lyophilized crude peptide were verified by reversed-phase high performance liquid chromatography analysis and mass-assisted laser desorption ionization time of flight mass spectrometry. The crude peptide was coupled to keyhole limpet hemocyanin via the heterobifunctional cross-linker sulfo-succinimidyl 4-*N*-maleimidomethyl cyclohexane 1-carboxylate. Rabbits (chinchilla bastards) were immunized with 400 μg of peptide conjugate at days 0, 14, 28, and 40. The first test serum was taken 6 weeks after the first boost. Preadsorbed βΔ7 antibody K12 was generated by overnight coincubation of serum (dilution 1:20) with a membrane preparation from HEK293 cells transfected with the β subunit.

Lysate and Membrane Preparation—For total cell lysates, transfected cells were lysed in 25 mM potassium phosphate buffer, pH 7.4, containing 5 mM EDTA and a protease inhibitor mixture (Roche). Membranes were separated from nuclei by ultracentrifugation (140,000 × *g* for 1 h). Pellets were resuspended in reducing sample buffer (2% SDS, 5% β-mercaptoethanol in 0.68 M Tris, pH 6.8) and separated on a 10% polyacrylamide gel (20 μl of lysate/lane). For membrane protein analysis, crude cell membranes were prepared from transfected cells and mouse tissues as described previously (36). For detection of myc-tagged β or βΔ7 the monoclonal and polyclonal anti-myc antibodies 9E10 (Santa Cruz) were used. The native β subunits were detected with the polyclonal anti-GlyRβ-(H170) antibody (Santa Cruz). For detection of the α subunits mAb4a hybridoma supernatant was used, for detection of gephyrin a monoclonal anti-gephyrin antibody (Clontech). Proteins were visualized using either horseradish peroxidase-conjugated goat anti-mouse IgG (Dianova) followed by detection using the ECL*Plus* system (GE Healthcare) or goat anti-rabbit IgG-Cy5 (Dianova) analyzed with fluoroimager STORM 860 (GE Healthcare).

Immunocytochemistry—Transfected COS7 cells grown on coverslips were fixed in 4% paraformaldehyde, 4% sucrose in phosphate-buffered saline for 10 min, washed twice in phosphate-buffered saline (1.5 mM KH_2PO_4, 6.5 mM Na_2HPO_4, 3 mM KCl, 137 mM NaCl), and blocked with 5% goat serum in phosphate-buffered saline for 30 min at room temperature, permeabilized, and incubated with primary antibody for 1 h at room temperature. After washing, the secondary antibody goat anti-rabbit IgG Alexa 488 (Dianova) (1:200) was applied for 1 h. Slides were analyzed using a confocal microscope (Leica).

Immunoprecipitation—Crude cell membranes (1 mg) were resuspended in 20 mM Tris-HCl, pH 7.0, and sodium desoxycholate (10% in 50 mM Tris-HCl, pH 9.0), and incubated for 30 min at 30 °C, followed by solubilization with 2% Triton X-100 in 50 mM Tris-HCl, pH 7.0, while gently agitating for an additional 30 min at 30 °C. After centrifugation (100,000 × *g*, 30 min), protein complexes were precipitated using polyclonal anti-myc antibody (1:100) by rotating the supernatants overnight at 4 °C. Prior to precipitation, a supernatant sample was harvested for further analysis. Protein complexes were incubated with protein A-conjugated Sepharose beads (Sigma). Following a 1-h incubation at 4 °C and three washing steps (20 mM Tris-HCl, pH 7.0, 0.16 M NaCl), the immunosorbent was collected at 3,000 × *g*. The precipitated proteins were eluted by heating at 95 °C for 5 min in 2× SDS sample buffer.

Topology Prediction—The topology of GlyR β and βΔ7 was predicted according to Expasy for post-translational modification. The prediction of transmembrane domains was based on a hidden Markov model (37, 38) and the predict protein server (39).

RESULTS

Single Cell RT-PCR Analysis of GlyR Expression in Rat Spinal Cord Glial Cells—The starting point of this study was the analysis of GlyR subunit transcripts in glial cells, as investigated in spinal cord slices of young rats (1–3 weeks old). The majority of cells were astrocytes as they showed passive membrane properties as revealed by their whole cell membrane currents (Fig. 1*A*, *G2*) (30, 34). A second population of cells exhibited voltage-dependent currents characteristic for glial progenitor or NG2 glial cells (Fig. 1*A*, *P1*). Because in some cells we also observed a small component of symmetrical decaying in- and outward potassium currents, we cannot exclude the inclusion of some oligodendrocytes in our study (not shown). Glycine-evoked currents were recorded by the patch clamp technique in the whole cell configuration (Fig. 1, *A* and *B*). Thereafter, cytoplasmic RNA was harvested by applying negative pressure to the patch pipette. Surprisingly, subsequent RT-PCR analysis using nested PCR with GlyR β-specific primers detected the expression of cDNA fragments of 356 bp, instead of 509 bp as expected from the known GlyR β subunit cDNA sequence (Fig. 1, *C* and *D*). cDNA sequencing of the subcloned fragments of 356 bp revealed a novel alternatively spliced variant of the GlyR β subunit lacking exon 7. This novel variant is designated GlyR βΔ7.

Deleted from the βΔ7 transcript, exon 7 encodes a region ranging from the C-terminal part of the large extracellular

Downloaded from http://www.jbc.org/ by guest on September 27, 2016

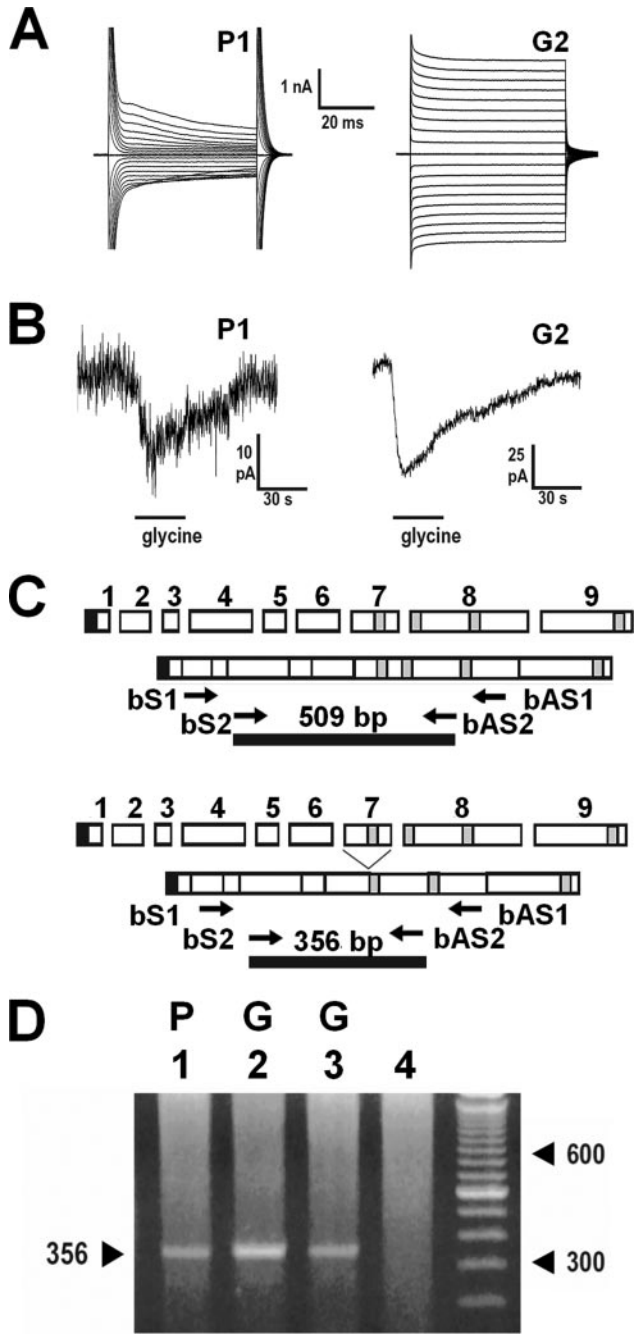

FIGURE 1. **Analysis of GlyRβ subunit expression in glial cells of the rat spinal cord by single cell RT-PCR.** A series of spinal cord glial cells were analyzed by patch clamp recording for their expression of glycine-evoked currents and subsequently investigated for the identification of GlyR β subunit encoding mRNAs. *A*, a series of de- and hyperpolarizing voltage steps (−160 to 20 mV) from a holding potential of −70 mV was applied and membrane currents were recorded. The delayed rectifying outward current activated at the depolarizing potential identifies cell number *1* as a precursor cell (P). The symmetrical pattern of in- and outward currents of cell number *2* reflects the current pattern of a mature glial cell (*G*). *B*, glycine (1 mM) applied while clamping the membrane potential at −70 mV evoked a whole cell inward current. *C*, primer selection for amplification of GlyR β transcripts. For the nested PCR approach two different primer pairs were selected from exons 2, 4, and 8. Using the primer pair bS2 and bAS2 a cDNA fragment of 509 bp for the full-length GlyR β is obtained, whereas cDNAs encoding GlyRβΔ7 give rise to a truncated fragment of 356 bp lacking the sequence region of exon 7. *D*, amplified cDNA fragments obtained from single cell RT-PCR of the precursor cell (*P*) and two mature glial cells (*G2* and *G3*) revealed a length of 356 bp employing GlyR β subunit-specific primers. *Lane 4* reflects the negative control of cytoplasmatic RNA obtained from glial cells displaying no glycine-evoked inward current.

domain, TM1 and the intracellular loop between TM1 and TM2 to the first four amino acid residues corresponding to TM2 (Fig. 2*A*). Analysis of the polypeptide variant encoded by the βΔ7 transcript predicted a primary structure where TM1 and the loop connecting TM1 and TM2 were missing, suggesting a dramatic change in subunit topology (Fig. 2, *B* and *C*). Moreover, four positions of the amino acids corresponding to the pore-forming TM2 were also missing. Based on hydrophobicity analysis, only two TMs were postulated for βΔ7, suggesting a loss of TM2 (Fig. 2*C*, *middle panel*). Rather, prediction of secondary structure (39) suggested that the remaining amino acid residues of the former TM2 substitute for the 10th β-sheet of the N-terminal domain that are lost by exon 7 deletion. Due to loss of exon 7, the secondary structure probability of the former TM2 positions changes from α-helical to β-strand, completing the fold of the acetylcholine-binding protein-like N-terminal domain (Fig. 2, *B* and *C*, *right panels*) (4, 19). Concurrently, the ion channel pore characteristic of the Cys-loop receptor subunits is lost in βΔ7.

To functionally characterize the βΔ7 polypeptide, we cloned the coding sequence into the eukaryotic expression vector pRK7. In addition, β and βΔ7 constructs were generated carrying an N-terminal c-myc epitope (9E10) recognized by specific antibodies (Fig. 2*A*).

Cell Type and Tissue Distribution of β Subunit Transcript Variants in Situ—Analysis of the tissue distribution of the major β subunit transcript variants was extended to spinal cord (sc), cerebral cortex (cx), heart (he), and liver (li) of adult mice (Fig. 3*A*). Cortex contained high levels of the novel βΔ7 splice variant, whereas liver and heart yielded a weak signal for this transcript. In adult spinal cord the signal for the read-through β transcript was barely detectable. Analysis of βΔ7 transcript distribution in embryonic, neonatal, and adult central nervous system revealed no significant developmental regulation (not shown).

Consistent with the single cell PCR data, RT-PCR analysis of β subunit transcripts present in primary astrocytes and neurons cultured from the mouse central nervous system confirmed the presence of the two major β subunit transcripts, corresponding to the read-through β transcript (606 bp) and the variant lacking exon 7 (453 bp) (Fig. 3*B*). In cultured astrocytes, the βΔ7 transcript prevailed, whereas the read-through β variant predominated in spinal cord neurons.

In Vivo Expression of βΔ7—To verify if the βΔ7 transcript is translated, membrane preparations from neuronal and non-neuronal tissues (cortex, spinal cord, and liver) were analyzed for concomitance of the read-through β subunit and the splice variant βΔ7 (Fig. 4). Using the commercial antibody H170 directed against GlyR β variants, we indeed detected an antigen of 53 kDa molecular mass in cortex, spinal cord, and liver corresponding to βΔ7 (Fig. 4*A*). The staining intensity of the presumptive βΔ7 was not significantly different from the full-length β antigen. As evident from an Endo H digest (Fig. 4*A*, *right panel*), the observed double bands do not represent glycosylated and unglycosylated forms of the full-length β variant. After the Endo H digest, both bands were still present, running in a slightly lower position than those of the non-digested preparation. For immunological discrimination of βΔ7 from the

Downloaded from http://www.jbc.org/ by guest on September 27, 2016

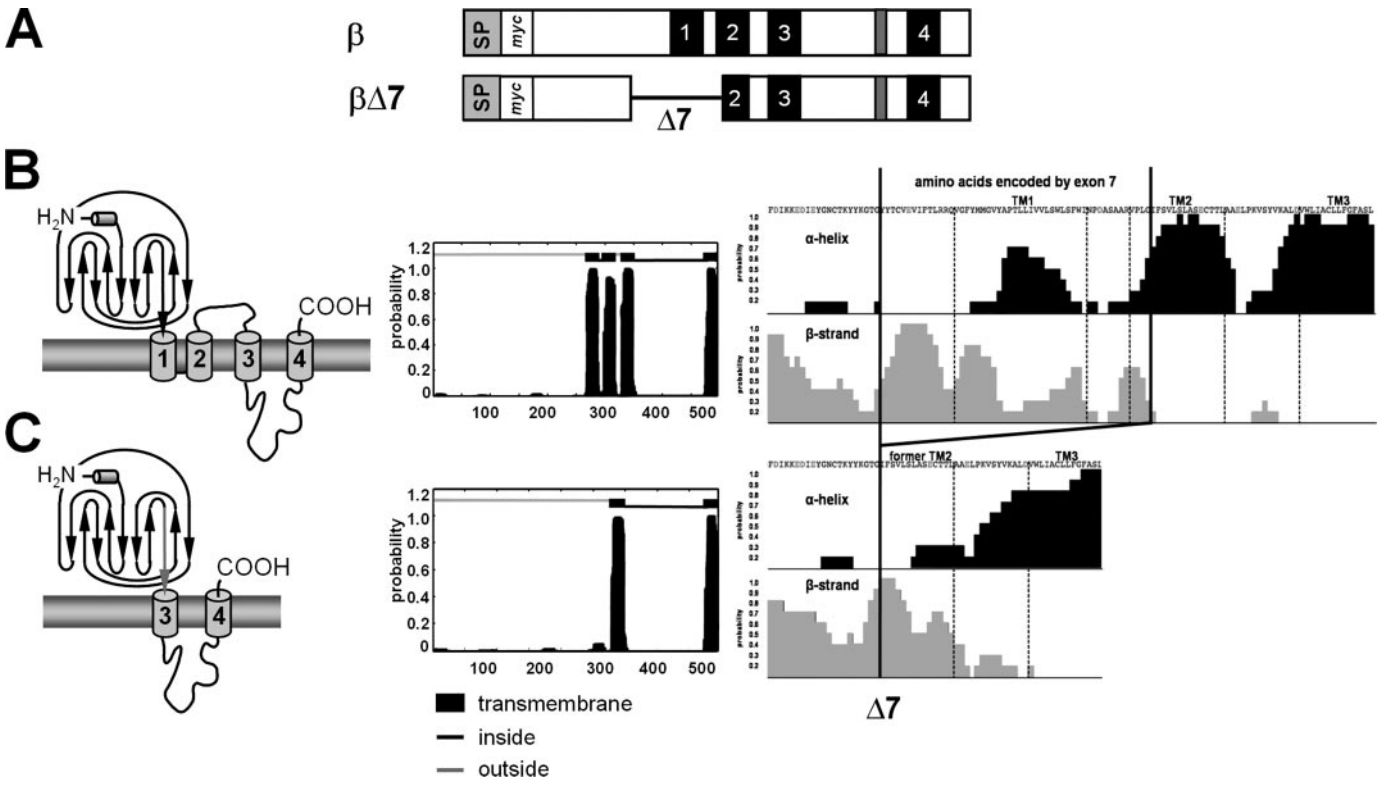

FIGURE 2. **Overall topology of GlyR β variants.** *A*, *bar diagram* representing both β and βΔ7 subunits used for *in vitro* studies. Following the signal peptide (*SP*), β subunits were N-terminal tagged with a myc epitope (9E10), *black boxes* represent transmembrane domains 1, 2, 3, and 4. *Black line* in βΔ7 shows localization of exon 7 deletion (amino acid positions 252–301). *Gray box* marks the binding motif for the anchor protein gephyrin of the GlyR complex at the postsynaptic membrane. *B*, topology models of the full-length β and βΔ7 subunits. *Left*, the β subunit is a member of the Cys-loop family of receptors with four transmembrane domains. The N terminus is highly homologous to the acetylcholine-binding protein, with a small α-helical domain followed by 10 β-sheets (*arrows*). *C*, proposed model of the βΔ7 splice variant. Due to exon deletion, the ion channel domain TM2 is lost and amino acids encoded by exon 8 replace the 10th β-sheet. *Middle*, topology prediction of β and βΔ7 based on hydrophobicity analysis. *Right*, secondary structure prediction for full-length β (Phe^{209}–Leu^{322}) and βΔ7 (Phe^{209}–Leu^{272}) proteins. The amino acid positions of the former TM2 domain of β switch from an α-helical structure into a β-strand in βΔ7.

read-through β variant, we generated a polyclonal antibody (K12) against the bridging epitope between exons 6 and 8 that is characteristic of the deletion variant. In membranes from transfected HEK cells, the βΔ7-specific antibody K12 recognized only the splice variant, but not the full-length β subunit (Fig. 4*B*). In membranes from mouse liver, a double band was detected, most likely representing additional heterogeneity, *e.g.* the presence of glycosylated and unglycosylated isoforms of βΔ7, or additional splice variants. Preadsorption of K12 against full-length β subunit antigen did not detectably alter the staining pattern, arguing for the specificity of K12 antiserum (Fig. 4*B*).

Cell Surface Expression of the Variants GlyR β and βΔ7—The topological model of βΔ7 predicted a deletion of structural elements that are essential for proper transmembrane folding of Cys-loop receptors of the nicotinic acetylcholine receptor superfamily (19). Thus, we asked whether the βΔ7 polypeptide was efficiently integrated into the plasma membrane. To this end, βΔ7 polypeptide was recombinantly expressed in the presence and absence of α1 subunits, and its subcellular distribution was determined by comparing intracellular and surface protein fractions (Fig. 5*A*). Surface proteins were labeled by biotinylation using sulfo-NHS-S-S-coupled biotin. Consistent with earlier reports, the α1 subunit of GlyR, detectable by monoclonal antibody mAb4a, was detected in both the intracellular and the cell surface fraction (Fig. 5*B*). The cytoplasmatic anchor protein of the GlyR complex, gephyrin, served as a control for the exclusion of cytoplasmatic protein from extracellular protein biotinylation (Fig. 5*B*).

Previous studies (40, 41) showed that an efficient plasma membrane integration of the GlyR β subunit requires a complex formation with ligand binding α subunits. Surprisingly, our experiments yielded a strong surface and intracellular expression signal for both, β (60 kDa) and βΔ7 (55 kDa) constructs, even when expressed alone (Fig. 5*A*). For each of the constructs, however, two bands of distinct molecular weights appeared. As the amino acid sequence of the β subunit harbors two extracellular glycosylation sites, this heterogeneity may be attributed to glycosylation (β, 56 kDa, and βΔ7, 51 kDa). Note that the smaller β subunit antigen of both variants is expressed at the cell surface in COS7 cells. Coexpression of both β variants with the α1 subunit did not significantly increase the relative abundance of the biotinylated surface fraction of the β and βΔ7 polypeptides (Fig. 5*A*).

Integration of the subunit variants β and βΔ7 into the plasma membrane of COS7 cells was also followed by immunocytochemistry (Fig. 5, *C* and *D*). As seen in permeabilized cells (Fig. 5*C*), the fraction of protein accumulating in intracellular compartments exceeded that of surface β protein (Fig. 5*D*). The subcellular distribution of tagged β antigens suggested that a large fraction of the intracellular β and βΔ7 variants were retained in the endoplasmic reticulum. Indeed, co-localization

Downloaded from http://www.jbc.org/ by guest on September 27, 2016

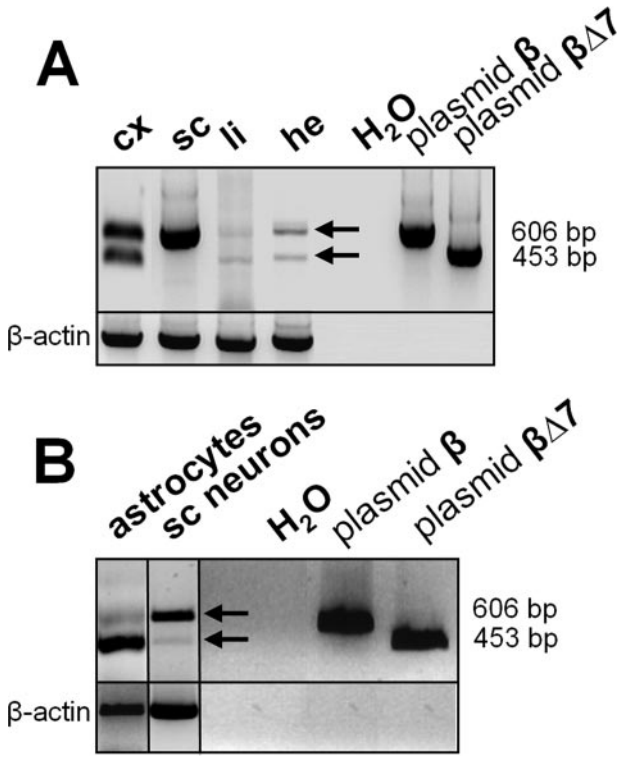

FIGURE 3. **Expression of β and βΔ7 transcripts in various tissues of mice.** *A*, cortex (*cx*), spinal cord (*sc*), heart (*he*), and liver (*li*) were used for β and βΔ7 transcript amplification. β-Actin (*lower panel*) was used as housekeeping gene, and reveals that the same amount of RNA was used for each probe. *B*, transcript level of βΔ7 in cultured astrocytes compared with spinal cord neurons. β and βΔ7 were amplified from plasmids (expected size of 606 and 453 bp) as control for the correct transcript size. Note the high amount of βΔ7 transcript observed in cultured glial cells at DIV 14 (cultured at P0).

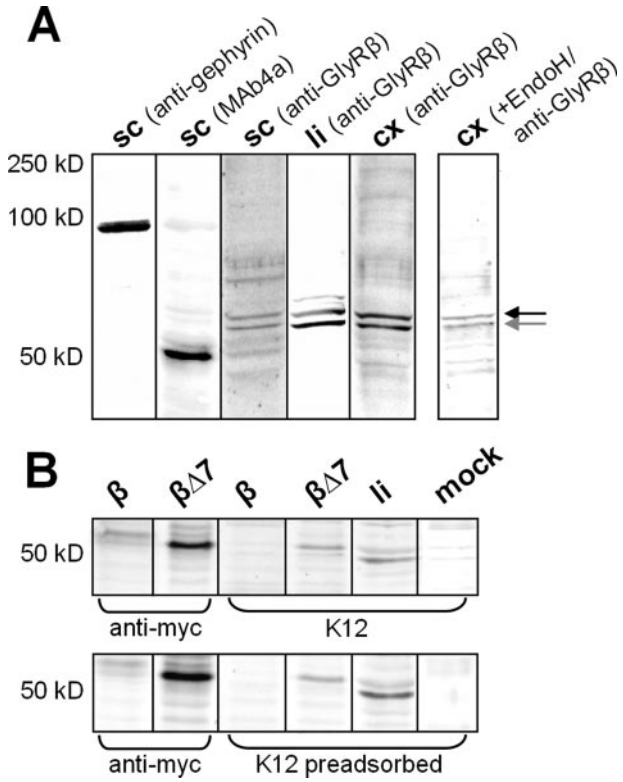

FIGURE 4. ***In vivo* protein expression of βΔ7 in different tissues.** *A*, membrane preparations from spinal cord (*sc*), cortex (*cx*), and liver (*li*) of adult mice. Positive controls: sc stained with monoclonal anti-gephyrin antibody for recognizing the 93-kDa anchor protein gephyrin (*first lane*) and with mAb4a to recognize the GlyR α1 subunit (*second lane*). Spinal cord, cortex, and liver were stained using the polyclonal anti-GlyR-β-H170 antibody, which recognizes an epitope in the intracellular TM3–4 loop of the GlyR β subunit. Cortex preparation was digested with Endo H. The *black arrow* points to the 58-kDa band of the β subunit; *gray arrow* to the 53-kDa signal of βΔ7. The positive control for Endo H digest is shown in Fig. 6*B*. *B*, antibody K12 specific for the splice variant βΔ7 recognizes an epitope bridging the exon 6/8 border. Membrane preparation from β- and βΔ7-transfected HEK cells, both constructs were stained with anti-myc antibody or K12 (1:100). K12 was tested on liver (*li*) and mock-transfected HEK cells compared to preadsorbed K12 antiserum.

with endoplasmic reticulum-specific proteins was confirmed by co-expression with DsRed-endoplasmic reticulum (not shown).

Glycosylation Studies on GlyR β and βΔ7—The extracellular domain carries two potential *N*-glycosylation consensus sequences (NX(S/T): NST^{54-56} and $NCT^{242-244}$), which may account for the polypeptide heterogeneity observed upon recombinant expression. Transfected COS7 cells were grown in the presence of tunicamycin, an inhibitor of formation of the core oligosaccharide. In tunicamycin-treated cells, only the low molecular weight species was present, indicating the unglycosylated forms of the β and βΔ7 polypeptides (Fig. 6*A*). Conversely, the larger molecular weight bands represent the glycosylated β and βΔ7 polypeptides. Glycosylation could also be demonstrated by sensitivity of the glycosylated polypeptides to Endo H. Indeed, when surface protein fractions were digested with Endo H, only the smaller species of βΔ7 was detected, consistent with an unglycosylated structure of the smaller polypeptide (Fig. 6*B*).

Association of βΔ7 with the α1 Polypeptide and Gephyrin—Clustering of GlyRs at the postsynaptic membrane depends on an interaction of a motif within the TM3–4 loop of the β subunit with the cytoplasmatic anchor protein gephyrin (8). For formation of molecular complexes in transfected HEK293 cells, βΔ7 polypeptide was analyzed in immunoprecipitation studies upon recombinant co-expression with the α1 subunit and gephyrin (ratio α1/β or βΔ7/gephyrin: 1/5/5). Using antibodies against the myc epitope of β or βΔ7 constructs, significant amounts of GlyRα1 polypeptide (Fig. 6*C*) and gephyrin (Fig. 6*D*) were co-immunoprecipitated. These data indicated that the βΔ7 polypeptide, despite its fundamentally altered transmembrane topology, is able to form molecular protein complexes with both, the α1 subunit and gephyrin.

Is There a Physiological Response of βΔ7?—Upon inclusion of the β subunit, heteromeric α1β chloride channels acquire a relative resistance to the plant toxin picrotoxin, which is absent from α1 homomers (23). Indeed, HEK293 cells transfected with α1 subunit cDNA yielded glycine-induced chloride currents sensitive to picrotoxin (19 ± 5% I_{max}), consistent with the formation of α1 homomers (Fig. 7, *A* and *D*). Despite the presence of picrotoxin, glycine currents were largely reconstituted upon co-transfection of the full-length β subunit (58 ± 11% I_{max}, Fig. 7, *B* and *D*). However, α1βΔ7 heteromers were efficiently blocked by picrotoxin (10 ± 2.4% I_{max}), indistinguishable from the situation in α1 homomeric receptor channels (Fig. 7, *C* and *D*). The glycine-gated maximal currents (I_{max}) of both heteromeric receptor complexes α1β and α1βΔ7, however, were

Downloaded from http://www.jbc.org/ by guest on September 27, 2016

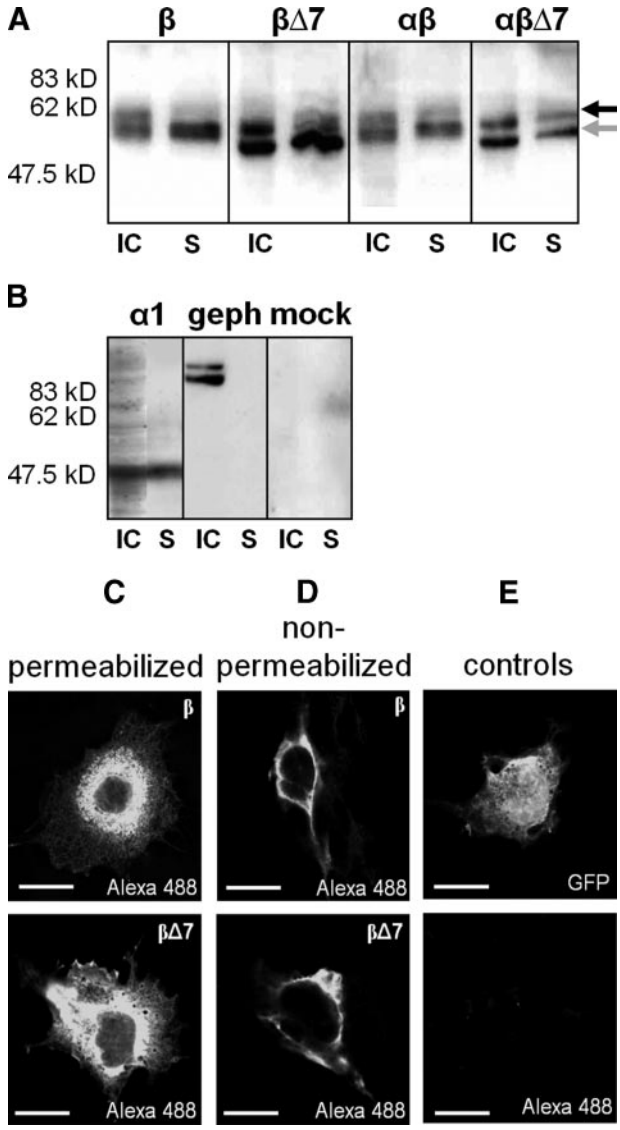

FIGURE 5. **Protein expression of βΔ7 in transfected COS7 cells.** *A*, both variants were expressed alone and in combination with the α1-subunit in COS7 cells (amount of DNA used: 5β:1α). Surface expression was analyzed by labeling membrane-embedded proteins with NHS-SS-biotin. Biotinylated proteins were bound to streptavidin-agarose beads followed by separation on 10% SDS gels. The amount of surface protein (*S*) was compared with intracellular non-labeled protein (*IC*) using the monoclonal anti-myc antibody, which recognizes the myc-tagged β subunits of the GlyR. The *black arrow* points to the 60-kDa band of β and 55 kDa of βΔ7. An additional lower band (*gray arrow*) represents the unglycosylated form of both β proteins (verified by Endo H digest, see Fig. 6*B*). α1 and gephyrin-transfected cells were used as controls (*B*), α1 shows that a high degree of surface integration, gephyrin (93 kDa), was found only in the intracellular probe. Green fluorescent protein-transfected COS7 cells were used as negative control. *C* and *D*, subcellular localization of β and βΔ7 in transfected COS7 cells after fixation with 4% paraformaldehyde + 4% sucrose. Cells were incubated with (permeabilized) (*C*) and without (non-permeabilized) Triton X-100 (*D*). Variants β and βΔ7 are highly expressed intracellular in the cytoplasm, but also at the cell surface. *E*, green fluorescent protein (*GFP*)-transfected cells and untransfected cells, stained only with secondary antibody. *Scale bar* represents 20 μm.

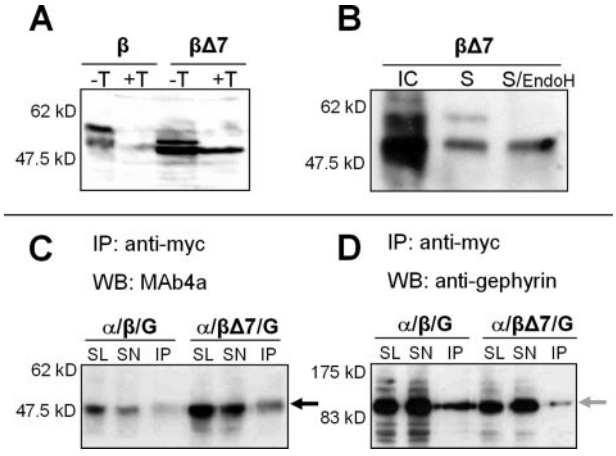

FIGURE 6. **Both GlyR β variants are glycosylated and form complexes with the α1 subunit and gephyrin.** *A*, cell lysates from β- and βΔ7-transfected COS7 cells were used for *N*-linked glycosylation analysis (−*T*, without tunicamycin). +*T*, treatment of cells with tunicamycin (5 μg/ml) for 24 h (added to the cells 5 h post-transfection. *B*, *IC*, intracellular fraction of βΔ7; *S*, surface protein labeled with biotin and detected using anti-myc 9E10 antibody. The surface fraction of βΔ7-transfected cells was digested with Endo H. *C* and *D*, protein complex formation of α1 and βΔ7 polypeptides with the cytosolic anchor protein gephyrin. Membrane preparations from transfected HEK293 cells were used for immunoprecipitation. β and βΔ7 were precipitated using the polyclonal myc antibody (1:100) and stained (*C*) with mAb4a for GlyRα subunits, solubilized protein (*SL*), supernatant after precipitation (*SN*), and precipitated fraction (*IP*). The *black arrow* points to the 48-kDa α1 subunit. *D*, protein complex formation of βΔ7 with the GlyR anchor protein gephyrin (dilution of antibody 1:200). The *gray arrow* marks the 93-kDa gephyrin.

reduced compared with α1 homomers (Fig. 7*E*). Although the formation of α1βΔ7 molecular protein complexes was clearly demonstrated, the novel subunit βΔ7 did not confer the important pharmacological property of picrotoxin resistance to the ion channel protein. These data suggest that the ion channel pore is homomeric and formed only by α1 subunits. This observation is consistent with the structural prediction that the deletion of exon 7 leads to the loss of a functional pore domain in βΔ7.

DISCUSSION

Here, we show that the rodent GlyR β subunit is alternatively spliced in neural and extraneural tissues. Compared with the read-through β subunit variant prevalent in adult spinal cord and cortex, the novel splice variant βΔ7 lacks exon 7, equivalent to a deletion of 51 amino acids. In the full-length subunit polypeptide, the deleted positions cover a segment of the N-terminal domain preceding membrane entry as well as the complete transmembrane domain TM1, the intracellular loop connecting TM1 and TM2, and the first four amino acids of the pore forming TM2.

Whereas functional GlyRs are formed by recombinant α subunit expression, homomeric expression of β subunits has not been seen to result in the efficient formation of glycine-gated anion channels (10). As evident from *in situ* hybridization (11), GlyR α and β subunit mRNAs show a disparate distribution in the rodent central nervous system, were α subunit transcripts predominate in spinal cord and brainstem. In contrast, β subunit mRNA is highly expressed throughout the central nervous system, including those forebrain regions that lack a significant α subunit transcription (11). Whereas the role of the regionally isolated expression of the β subunit is not understood, increasing evidence indicates that this subunit also occurs in non-neuronal cells, including astroglia, oligodendrocytes, and glial progenitor cells/NG2-glia (30).

At the transcript level, the subunit variant βΔ7 was highly expressed in glial cells and non-neuronal tissues, but less abun-

Downloaded from http://www.jbc.org/ by guest on September 27, 2016

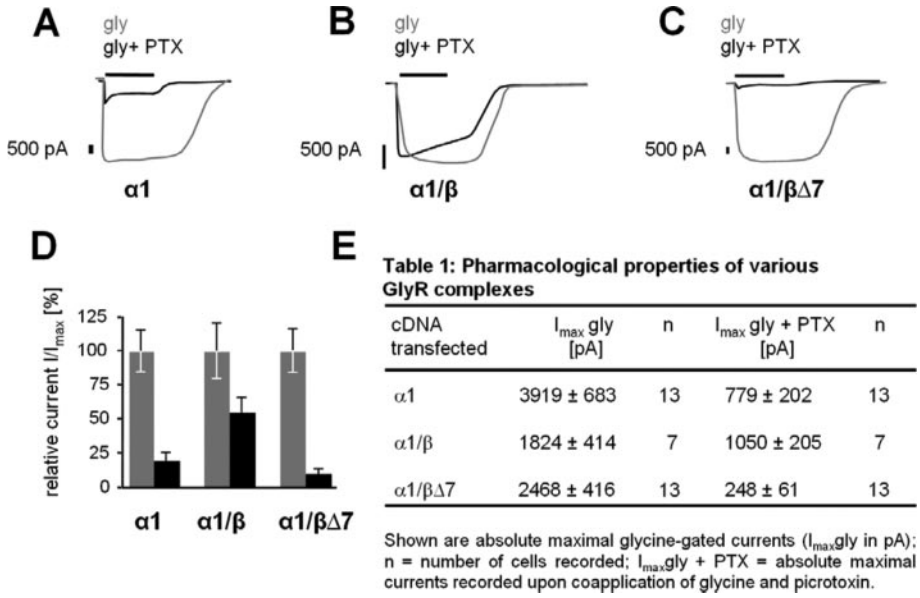

Table 1: Pharmacological properties of various GlyR complexes

cDNA transfected	I_{max} gly [pA]	n	I_{max} gly + PTX [pA]	n
α1	3919 ± 683	13	779 ± 202	13
α1/β	1824 ± 414	7	1050 ± 205	7
α1/βΔ7	2468 ± 416	13	248 ± 61	13

Shown are absolute maximal glycine-gated currents (I_{max}gly in pA); n = number of cells recorded; I_{max}gly + PTX = absolute maximal currents recorded upon coapplication of glycine and picrotoxin.

FIGURE 7. **Heteromeric α1/βΔ7 complexes are indistinguishable from α1 homomers.** HEK293 cells were transfected with α1:β:gephyrin or α1:βΔ7:gephyrin 1:5:5. Glycine-gated maximal currents (I_{max}) were obtained holding the cell at −60 mV, glycine was applied for 2 s. Glycine concentration of 100 ± 100 μM picrotoxin was used to distinguish between α1 homomers and α1/β heteromers. Picrotoxin is known to block α1-homomeric receptor complexes, verified also in *A*. *B*, αβ-heteromeric complexes show almost no effect by picrotoxin due to a different pentameric pore-forming TM2 composition. *C*, α/βΔ7, heteromers are blocked to about 90% by picrotoxin and are indistinguishable from α1-homomers although the current left after picrotoxin block is even more decreased than with α1 homomers. *D*, *bar diagram* representing relative currents I/I_{max} [%]. Glycine-gated currents recorded from transfected HEK293 cells with α1 alone, αβ, or αβΔ7 were set to 100% (*black bars*). *Gray bars* demonstrate the percentage of block by picrotoxin. *E*, summarized physiological properties from electrophysiological recordings.

dant in neurons. Among the tissues transcribing the *Glrb* gene, the variant βΔ7 was found in a subset of cells and tissues. Astrocytes were the most abundant cell type, playing a fundamental role in maintenance of the extracellular microenvironment during neuronal activity (42). The splice variant βΔ7 was highly transcribed in cerebral cortex and extraneural tissues like heart and liver, but hardly detectable in spinal cord. Whereas splicing of β subunit pre-mRNA into the β and βΔ7 variant was tissue selective, no evidence was obtained for a developmental regulation. This situation clearly differs from the strict developmental regulation of GlyR α subunit variants in the central nervous system (11, 41, 43). Spatial expression patterns of central nervous system proteins may not only be attributed to tissue-specific transcription, but also result from a tissue-specific splicing. The neurooncological ventral antigen-1 (Nova-1) is a regulator of neuronal pre-mRNA splicing that contributes to the regulation of GlyR α2 variants in immature neurons (44). Similar processes may also apply to the regional regulation of β pre-mRNAs.

Sequence analysis of the GlyR splice variant βΔ7 predicted a non-canonical topology of this Cys-loop receptor subunit. Rather than four transmembrane regions, sequence analysis of the βΔ7 variant predicted two membrane spanning segments. In contrast, the two Cys-loops located in the extracellular N-terminal domain that are characteristic of the GlyR family (4), are conserved in the splice variant βΔ7. This fundamental alteration in predicted transmembrane topology gives rise to the question whether the βΔ7 variant is translated into a functional polypeptide that undergoes membrane integration and assembles into functional GlyR ion channel complexes. As detectable in the mouse central nervous system *in vivo*, presence of the βΔ7 transcript variant correlated with a distinct β subunit antigen of slightly lower molecular weight, suggesting that this splice variant is stably translated in cerebral cortex and extraneural tissues.

Hetero-oligomeric GlyRs are ion channel protein complexes with a subunit stoichiometry of $\alpha_2\beta_3$, where the β subunit contributes to the formation of the ligand binding site at its interface to the α subunit (19). In Cys-loop receptors, neurotransmitter binding is believed to require discontinuous segments of the N-terminal extracellular regions of two adjacent subunits, situated in a distance of ~30 Å from the membrane (45). The amino acid positions proposed to delineate the ligand binding site are not affected by the deletion characteristic of βΔ7. Secondary structure prediction suggests that the amino acids remaining from the former α-helix of TM2 structurally replace those amino acids forming the 10th β-sheet of the N-terminal domain of the full-length β peptide. Similar changes from an α-helix into a β-sheet stretch are also known from other proteins, *e.g.* β-amyloid or prion proteins (46). The integration of the amino acid residues remaining from TM2 into the secondary structure of the N-terminal domain implies the loss of the ion channel domain.

Both, the novel subunit variant βΔ7, as well as the read-through β polypeptide, were sorted into the plasma membrane of COS7 cells, even in the absence of the ligand binding α1 subunit. Consistent with a stable expression of the βΔ7 polypeptide, its assembly properties were indistinguishable from those of the full-length GlyR β subunit. In mature neurons, the read-through β subunit polypeptide interacts with both, the ligand binding GlyR α subunit and the postsynaptic anchor protein, gephyrin. The latter protein plays an important role for anchoring of both, glycine and $GABA_A$ receptors (8, 47, 48). By a sorting process mediated by gephyrin, α/β heteroligomeric receptors are targeted to the postsynaptic membrane (49). Likewise, recombinant βΔ7 polypeptide formed a stable molecular complex with both, the α1 subunit polypeptide and gephyrin, as evident from co-immunoprecipitation with a tagged βΔ7 construct. This interaction with the cytosolic protein gephyrin also suggested that the TM3–4 loop was localized intracellularly. The deletion of exon 7 does not significantly affect the assembly of hetero-oligomeric GlyR protein complexes, consistent with the identification of "assembly boxes" (40), *i.e.* amino acid motives located in the highly conserved N-terminal regions that are not affected by the βΔ7 dele-

Downloaded from http://www.jbc.org/ by guest on September 27, 2016

tion. Still, the quaternary structure of $\alpha/\beta\Delta7$ complexes remains to be elucidated.

Whereas the post-transcriptional modification of β transcripts enhances the diversity of GlyR β subunit variants, the functional role of the $\beta\Delta7$ polypeptide remains unknown. In contrast to the read-through β subunit, which confers resistance to picrotoxin onto GlyR ion channels (3, 23, 24), our electrophysiological data show that $\beta\Delta7$ is not able to efficiently alter ion channel properties. Given the predicted loss of TM2, $\beta\Delta7$ represents a GlyR subunit variant that is no longer able to form a Cl^- channel pore. Rather, $\beta\Delta7$ may act as an accessory subunit of the GlyR complex, potentially contributing to the formation of larger protein complexes and membrane anchoring.

In addition to their classical role as ligand-gated chloride channels of the postsynapse, electrophysiological studies have demonstrated functional expression of GlyR chloride channels (50) and $GABA_A$ receptors (51) in astrocytes and other non-synaptic cells. Due to a lack of synaptic interactions of these cells, ligand-gated ion channels have been proposed to be involved in other functions, such as regulation of cell volume (52), pH (53), and cell proliferation (54). Given their role as interaction partners of gephyrin, GlyR β variants may also contribute to the cellular membrane architecture, independent of the ion channel function (11, 55, 56).

In addition to the physiological splice variants of the GlyR β subunit gene, pathological alterations in GlyR β pre-mRNA splicing underlie the human neurological disorder *hyperekplexia* and the *spastic* mutant of the mouse. In a case of *hyperekplexia* associated with a compound heterozygotic mutation of the *GLRB* gene, a splice mutation was found to cause a loss of exon 5 from β subunit transcripts (16). In *spastic* mice, insertion of a LINE-1 transposable element into intron 5 of the *Glrb* results in a dramatic reduction in full-length β transcripts (18, 57), producing a loss of GlyRs from spinal cord and brainstem. These observations underline the crucial role of the GlyR β subunit for a correct assembly and membrane insertion of GlyRs *in vivo*. Taken together, it has become apparent that alternative splicing contributes to the subtype heterogeneity of neurotransmitter receptors in the central nervous system.

Acknowledgments—We thank Dr. Cornel Mülhardt and Dr. Andrea Pastor-Zacharias for contributions during the initial phase of this study and Dagmar Zunner for generating tagged receptor constructs. Dr. Kristina Becker, Dr. Ralf Enz, and Nima Yazdkhasti are gratefully acknowledged for support and helpful discussions. Rosa Weber and Marina Wenzel provided excellent technical assistance.

REFERENCES

1. Lester, H. A., Dibas, M. I., Dahan, D. S., Leite, J. F., and Dougherty, D. A. (2004) *Trends Neurosci.* **27,** 329–336
2. Corringer, P. J., Le Novere, N., and Changeux, J. P. (2000) *Annu. Rev. Pharmacol. Toxicol.* **40,** 431–458
3. Langosch, D., Thomas, L., and Betz, H. (1988) *Proc. Natl. Acad. Sci. U. S. A.* **85,** 7394–7398
4. Brejc, K., van Dijk, W. J., Klaassen, R. V., Schuurmans, M., van Der Oost, J., Smit, A. B., and Sixma, T. K. (2001) *Nature* **411,** 269–276
5. Kim, E. Y., Schrader, N., Smolinsky, B., Bedet, C., Vannier, C., Schwarz, G., and Schindelin, H. (2006) *EMBO J.*, in press
6. Kneussel, M., Hermann, A., Kirsch, J., and Betz, H. (1999) *J. Neurochem.* **72,** 1323–1326
7. Meier, J., Vannier, C., Serge, A., Triller, A., and Choquet, D. (2001) *Nat. Neurosci.* **4,** 253–260
8. Meyer, G., Kirsch, J., Betz, H., and Langosch, D. (1995) *Neuron* **15,** 563–572
9. Sola, M., Bavro, V. N., Timmins, J., Franz, T., Ricard-Blum, S., Schoehn, G., Ruigrok, R. W., Paarmann, I., Saiyed, T., O'Sullivan, G. A., Schmitt, B., Betz, H., and Weissenhorn, W. (2004) *EMBO J.* **23,** 2510–2519
10. Grenningloh, G., Pribilla, I., Prior, P., Multhaup, G., Beyreuther, K., Taleb, O., and Betz, H. (1990) *Neuron* **4,** 963–970
11. Malosio, M. L., Marqueze-Pouey, B., Kuhse, J., and Betz, H. (1991) *EMBO J.* **10,** 2401–2409
12. Akagi, H., Hirai, K., and Hishinuma, F. (1991) *Neurosci. Res.* **11,** 28–40
13. Becker, C. M., Hoch, W., and Betz, H. (1988) *EMBO J.* **7,** 3717–3726
14. Meier, J. C., Henneberger, C., Melnick, I., Racca, C., Harvey, R. J., Heinemann, U., Schmieden, V., and Grantyn, R. (2005) *Nat. Neurosci.* **8,** 736–744
15. Nikolic, Z., Laube, B., Weber, R. G., Lichter, P., Kioschis, P., Poustka, A., Mulhardt, C., and Becker, C. M. (1998) *J. Biol. Chem.* **273,** 19708–19714
16. Rees, M. I., Lewis, T. M., Kwok, J. B., Mortier, G. R., Govaert, P., Snell, R. G., Schofield, P. R., and Owen, M. J. (2002) *Hum. Mol. Genet.* **11,** 853–860
17. Kingsmore, S. F., Giros, B., Suh, D., Bieniarz, M., Caron, M. G., and Seldin, M. F. (1994) *Nat. Genet.* **7,** 136–141
18. Mulhardt, C., Fischer, M., Gass, P., Simon-Chazottes, D., Guenet, J. L., Kuhse, J., Betz, H., and Becker, C. M. (1994) *Neuron* **13,** 1003–1015
19. Grudzinska, J., Schemm, R., Haeger, S., Nicke, A., Schmalzing, G., Betz, H., and Laube, B. (2005) *Neuron* **45,** 727–739
20. Kuhse, J., Schmieden, V., and Betz, H. (1990) *J. Biol. Chem.* **265,** 22317–22320
21. Kuhse, J., Schmieden, V., and Betz, H. (1990) *Neuron* **5,** 867–873
22. Hawthorne, R., and Lynch, J. W. (2005) *J. Biol. Chem.* **280,** 35836–35843
23. Pribilla, I., Takagi, T., Langosch, D., Bormann, J., and Betz, H. (1992) *EMBO J.* **11,** 4305–4311
24. Shan, Q., Haddrill, J. L., and Lynch, J. W. (2001) *J. Neurochem.* **76,** 1109–1120
25. Meier, J., and Grantyn, R. (2004) *J. Neurosci.* **24,** 1398–1405
26. Sassoe-Pognetto, M., Kirsch, J., Grunert, U., Greferath, U., Fritschy, J. M., Mohler, H., Betz, H., and Wassle, H. (1995) *J. Comp. Neurol.* **357,** 1–14
27. Todd, A. J. (1996) *Eur. J. Neurosci.* **8,** 2492–2498
28. van Zundert, B., Castro, P., and Aguayo, L. G. (2005) *Brain Res.* **1050,** 40–47
29. Wassle, H., Koulen, P., Brandstatter, J. H., Fletcher, E. L., and Becker, C. M. (1998) *Vision Res.* **38,** 1411–1430
30. Kirchhoff, F., Mulhardt, C., Pastor, A., Becker, C. M., and Kettenmann, H. (1996) *J. Neurochem.* **66,** 1383–1390
31. Lambolez, B., Audinat, E., Bochet, P., Crepel, F., and Rossier, J. (1992) *Neuron* **9,** 247–258
32. Chen, C., and Okayama, H. (1987) *Mol. Cell. Biol.* **7,** 2745–2752
33. Hamill, O. P., Marty, A., Neher, E., Sakmann, B., and Sigworth, F. J. (1981) *Pflugers Arch.* **391,** 85–100
34. Matthias, K., Kirchhoff, F., Seifert, G., Huttmann, K., Matyash, M., Kettenmann, H., and Steinhauser, C. (2003) *J. Neurosci.* **23,** 1750–1758
35. Ren, Z., Riley, N. J., Needleman, L. A., Sanders, J. M., Swanson, G. T., and Marshall, J. (2003) *J. Biol. Chem.* **278,** 52700–52709
36. Sontheimer, H., Becker, C. M., Pritchett, D. B., Schofield, P. R., Grenningloh, G., Kettenmann, H., Betz, H., and Seeburg, P. H. (1989) *Neuron* **2,** 1491–1497
37. Krogh, A., Larsson, B., von Heijne, G., and Sonnhammer, E. L. (2001) *J. Mol. Biol.* **305,** 567–580
38. Sonnhammer, E. L., von Heijne, G., and Krogh, A. (1998) *Proc. Int. Conf. Intell. Syst. Mol. Biol.* **6,** 175–182
39. Rost, B., Yachdav, G., and Liu, J. (2004) *Nucleic Acids Res.* **32,** W321–W326
40. Griffon, N., Buttner, C., Nicke, A., Kuhse, J., Schmalzing, G., and Betz, H. (1999) *EMBO J.* **18,** 4711–4721
41. Lynch, J. W. (2004) *Physiol. Rev.* **84,** 1051–1095
42. Zhang, X. D., Morishima, S., Ando-Akatsuka, Y., Takahashi, N., Nabekura,

Downloaded from http://www.jbc.org/ by guest on September 27, 2016

T., Inoue, H., Shimizu, T., and Okada, Y. (2004) *Glia* **47,** 46–57
43. Betz, H. (1991) *Trends Neurosci.* **14,** 458–461
44. Kumar, D. V., Nighorn, A., and St. John, P. A. (2002) *J. Neurobiol.* **52,** 156–165
45. Unwin, N. (2003) *FEBS Lett.* **555,** 91–95
46. Ross, E. D., Minton, A., and Wickner, R. B. (2005) *Nat. Cell Biol.* **7,** 1039–1044
47. Kirsch, J., and Betz, H. (1995) *J. Neurosci.* **15,** 4148–4156
48. Kirsch, J., Meyer, G., and Betz, H. (1996) *Mol. Cell. Neurosci.* **8,** 93–98
49. Kneussel, M., and Betz, H. (2000) *J. Physiol.* (*Lond.*) **525,** 1–9
50. Pastor, A., Chvatal, A., Sykova, E., and Kettenmann, H. (1995) *Eur. J. Neurosci.* **7,** 1188–1198
51. Fraser, D. D., Mudrick-Donnon, L. A., and MacVicar, B. A. (1994) *Glia* **11,** 83–93
52. Jackson, P. S., and Strange, K. (1993) *Am. J. Physiol.* **265,** C1489–1500
53. Makara, J. K., Petheo, G. L., Toth, A., and Spat, A. (2001) *Glia* **34,** 52–58
54. Rouzaire-Dubois, B., Milandri, J. B., Bostel, S., and Dubois, J. M. (2000) *Pflugers Arch.* **440,** 881–888
55. Kneussel, M., and Betz, H. (2000) *Trends Neurosci.* **23,** 429–435
56. Rees, M. I., Harvey, K., Ward, H., White, J. H., Evans, L., Duguid, I. C., Hsu, C. C., Coleman, S. L., Miller, J., Baer, K., Waldvogel, H. J., Gibbon, F., Smart, T. G., Owen, M. J., Harvey, R. J., and Snell, R. G. (2003) *J. Biol. Chem.* **278,** 24688–24696
57. Becker, C. M., Schmieden, V., Tarroni, P., Strasser, U., and Betz, H. (1992) *Neuron* **8,** 283–289

Downloaded from http://www.jbc.org/ by guest on September 27, 2016

A Novel Glycine Receptor β Subunit Splice Variant Predicts an Unorthodox Transmembrane Topology: ASSEMBLY INTO HETEROMERIC RECEPTOR COMPLEXES

Jana Oertel, Carmen Villmann, Helmut Kettenmann, Frank Kirchhoff and Cord-Michael Becker

J. Biol. Chem. 2007, 282:2798-2807.
doi: 10.1074/jbc.M608941200 originally published online December 4, 2006

Access the most updated version of this article at doi: 10.1074/jbc.M608941200

Alerts:
- When this article is cited
- When a correction for this article is posted

Click here to choose from all of JBC's e-mail alerts

This article cites 54 references, 14 of which can be accessed free at
http://www.jbc.org/content/282/5/2798.full.html#ref-list-1

Downloaded from http://www.jbc.org/ by guest on September 27, 2016